

Microstructure of $\text{In}_x\text{Ga}_{1-x}\text{N}$ nanorods grown by molecular beam epitaxy

R F Webster¹, Q Y Soundararajah¹, I J Griffiths¹, D Cherns¹,
S V Novikov² and C T Foxon²

¹H H Wills Physics Laboratory, University of Bristol, Tyndall Avenue, Bristol, BS8 1TL, UK

²School of Physics and Astronomy, University of Nottingham, Nottingham NG7 2RD, UK

E-mail: richard.webster@bristol.ac.uk

Received 14 April 2015, revised 30 July 2015

Accepted for publication 31 July 2015

Published 15 October 2015



CrossMark

Abstract

Transmission electron microscopy is used to examine the structure and composition of $\text{In}_x\text{Ga}_{1-x}\text{N}$ nanorods grown by plasma-assisted molecular beam epitaxy. The results confirm a core-shell structure with an In-rich core and In-poor shell resulting from axial and lateral growth sectors respectively. Atomic resolution mapping by energy-dispersive x-ray microanalysis and high angle annular dark field imaging show that both the core and the shell are decomposed into Ga-rich and In-rich platelets parallel to their respective growth surfaces. It is argued that platelet formation occurs at the surfaces, through the lateral expansion of surface steps. Studies of nanorods with graded composition show that decomposition ceases for $x \geq 0.8$ and the ratio of growth rates, shell:core, decreases with increasing In concentration.

Keywords: III-nitrides, molecular beam epitaxy, characterization, nanostructures

(Some figures may appear in colour only in the online journal)


Introduction

$\text{In}_x\text{Ga}_{1-x}\text{N}$ alloys with high In content are of great interest for solar cells and light emitting diodes operating at longer wavelengths. However, the efficiency of these devices falls as the In content increases. The reason for this deterioration in properties is not clear, but may involve a combination of factors including misfit and threading dislocations and the thermodynamic instability of $\text{In}_x\text{Ga}_{1-x}\text{N}$ alloys [1]. In previous work, we have used transmission electron microscopy (TEM) to examine the structure of $\text{In}_x\text{Ga}_{1-x}\text{N}$ nanorods grown on Si substrates by molecular beam epitaxy [2, 3]. Such nanorods are of great interest, as they can, in principle, be grown free of extrinsic defects (dislocations and planar faults) and the geometry allows partial elastic relaxation of misfit stresses. The TEM studies have confirmed that $\text{In}_x\text{Ga}_{1-x}\text{N}$ nanorods can be grown free of extrinsic defects for a range of compositions [2]. However, detailed

studies of $\text{In}_{0.5}\text{Ga}_{0.5}\text{N}$ nanorods have shown fine scale variations in composition leading to a core-shell structure with a Ga-rich shell and a generally In-rich core which itself is separated into In-rich and Ga-rich regions [3]. In this paper we report more recent studies where the In content of the nanorod has been varied. The results show how both decomposition and the core-shell structure vary with In content and that decomposition can occur in the shell as well as the core. These results are used to throw new light on the growth and decomposition mechanisms.

Experimental

$\text{In}_x\text{Ga}_{1-x}\text{N}$ nanorods were grown in a Varian ModGen II MBE system, with active nitrogen provided by an HD25 RF activated plasma source. Growth was carried out directly onto p-Si(111) substrates under strongly N-rich conditions. Substrate temperatures were in the range 400–500 °C to minimize desorption of the more volatile In species. The substrate was rotated at 10 revolutions/min with the In and Ga sources inclined at equal angles $\sim 35^\circ$. Samples were grown with

 Content from this work may be used under the terms of the Creative Commons Attribution 3.0 licence. Any further distribution of this work must maintain attribution to the author(s) and the title of the work, journal citation and DOI.

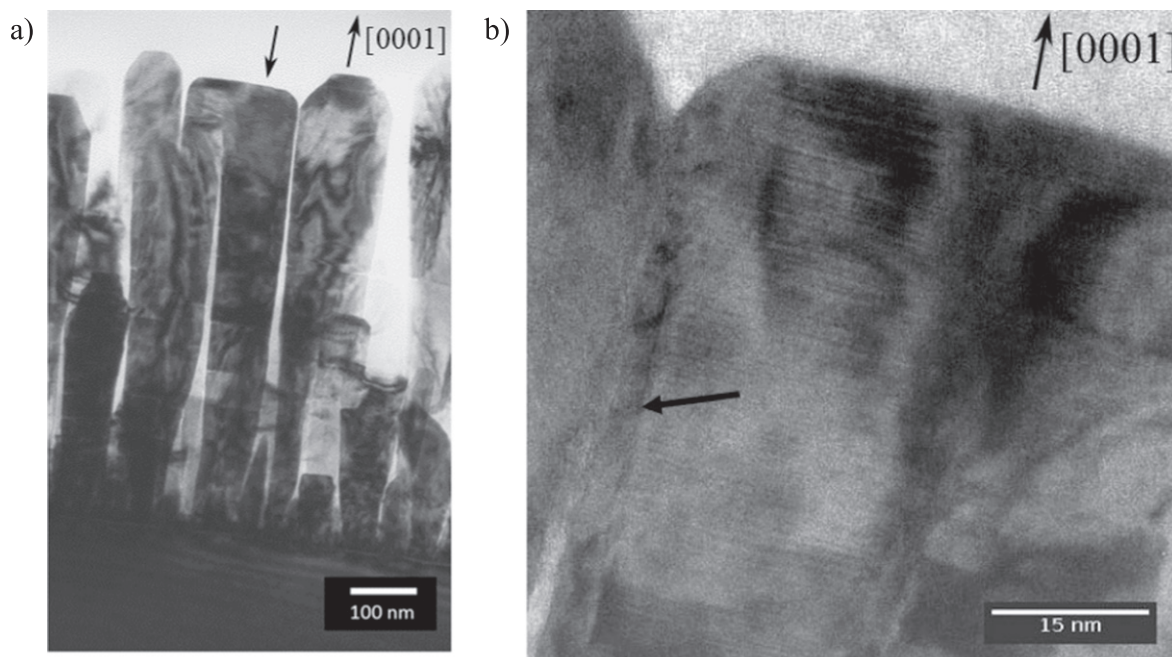


Figure 1. TEM images of a cross-sectional $\text{In}_{0.5}\text{Ga}_{0.5}\text{N}$ sample, (a) low magnification view, (b) higher resolution image showing a core-shell structure with decomposition in the core extending to the (0001) growth surface, and a tapered shell (arrowed) showing no apparent decomposition.

fixed values of x (ungraded samples) and with variable x (graded samples). Cross-sectional specimens were prepared for TEM both by mechanically scraping off nanorods onto holey carbon films and by mechanical polishing and Ar^+ ion beam thinning methods. Specimens in plan-view orientation were also prepared by gluing wafers together with a conducting epoxy resin and sectioning across nanorods using a FEI Helios Dual-beam focussed ion beam instrument; to minimize damage, thinning was carried out initially with 30 kV Ga ions, with a final polish at 5 kV.

Results and interpretation

Figure 1 shows cross-sectional bright field TEM images, taken using a JEOL 2010 microscope, of $\text{In}_{0.5}\text{Ga}_{0.5}\text{N}$ nanorods in a specimen prepared by mechanical polishing and ion thinning. In these images, the nanorods, which have the hexagonal wurtzite structure and grow along the [0001] direction, are seen with the (0002) planes close to edge-on. Figure 1(b) shows a higher magnification image from the top of the nanorod arrowed in figure 1(a). The strong banding seen running parallel to the trace of the (0002) plane is indicative of decomposition into alternate Ga-rich and In-rich platelets, seen more clearly in high angle annular dark field (HAADF) images, as discussed below. Such banding is not seen in a surrounding shell region (arrowed), which is seen to taper towards the top surface of the nanorod. A close examination shows that the banding (decomposition) in the core extends right to the top surface of the nanorod. As discussed later, the top of the nanorod also has side facets in a semi-

polar orientation, as do the other nanorods in figure 1(a) to a greater or lesser extent.

Figures 2(a), (b) illustrate images taken in the JEOL ARM 200F from a plan-view and cross-sectional image respectively. The plan-view image shows that the sectioned nanorods mostly have a hexagonal cross-section with {10-10} side facets. Figure 2(a) shows elemental mapping of the Ga-K and In-L peaks, illustrating the existence for a group of nanorods of distinct shell and core regions in which the In concentration was less (shell) and more (core) than the nominal composition ($x = 0.5$). Figure 2(b) is a HAADF image showing the core itself is separated into alternate In-poor and In-rich platelets, which are the dark and light bands respectively.

Detailed studies of both plan-view and cross-sectional samples showed evidence for decomposition in the shell as well as the core, but on {10-10} planes rather than on the (0002) planes as in figure 2(b). Figure 3 shows a HAADF image from a plan-view sample where the less bright contrast in the shell, compared with the core, is indicative of a generally lower In content, as seen in figure 2. Dark lines running parallel to {10-10} traces in the shell (2 of which are arrowed) can be tentatively interpreted as relatively Ga-rich platelets. This is confirmed by the EDX profiles, in figure 3(b), which show peaks in the Ga and troughs in the In signals at these points. HAADF from cross-sectional samples, as in figure 4, show these Ga-rich platelets (arrowed) extending down the length of the nanorods on (10-10) planes.

The observation of Ga-rich platelets in the shell throws new light on the decomposition mechanism. As these platelets lie in {10-10} orientation, contrasting with the (0001) orientation of platelets in the core, we can assume that the

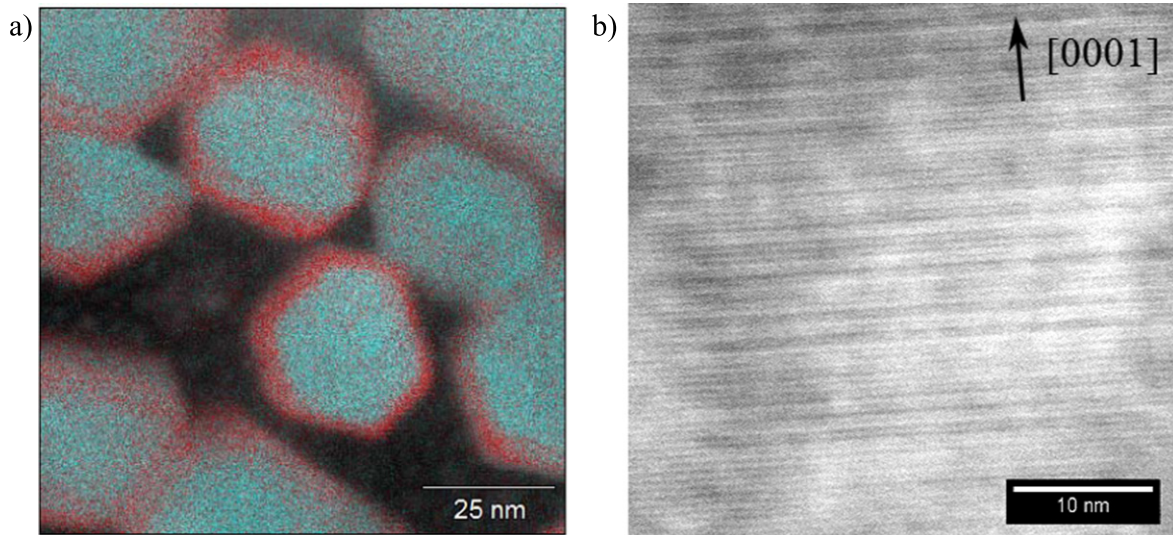


Figure 2. An $\text{In}_{0.5}\text{Ga}_{0.5}\text{N}$ sample (a) plan-view image showing a Ga-rich shell (red) and In-rich core (blue), (b) HAADF image of a cross-sectional sample showing the (0002) atomic planes edge-on, with variations in intensity indicating planes which are more Ga- or In-rich (In-rich planes show brighter contrast).

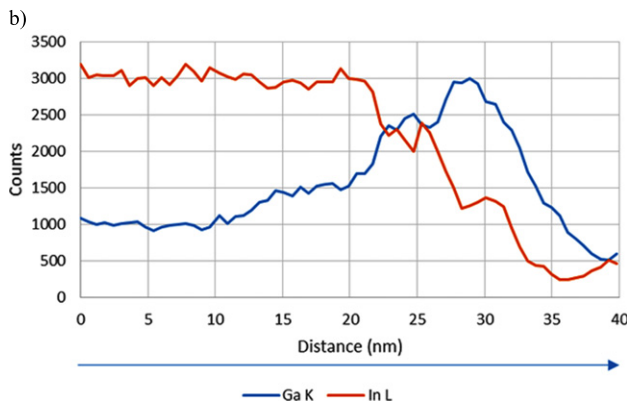
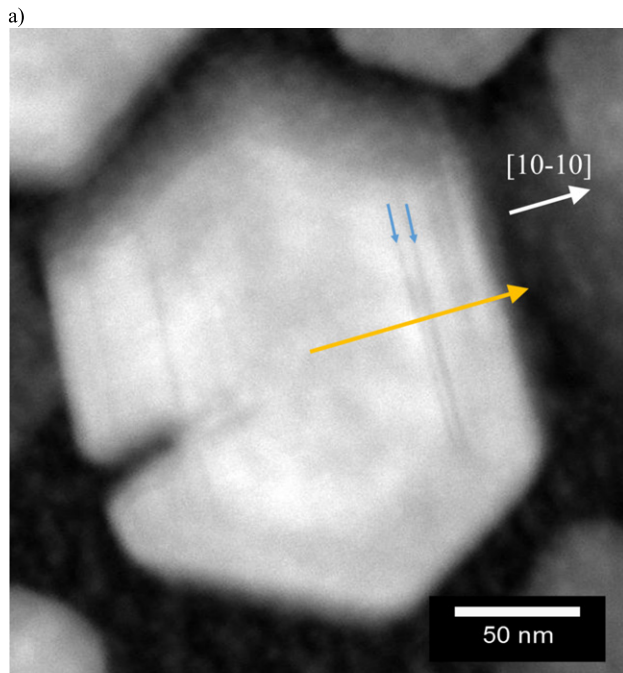


Figure 3. An $\text{In}_{0.5}\text{Ga}_{0.5}\text{N}$ sample (a) plan-view image showing dark bands, two of which are arrowed, (b) EDX linescan in the arrowed $\langle 10\text{-}10 \rangle$ direction showing the dark bands are relatively Ga-rich.

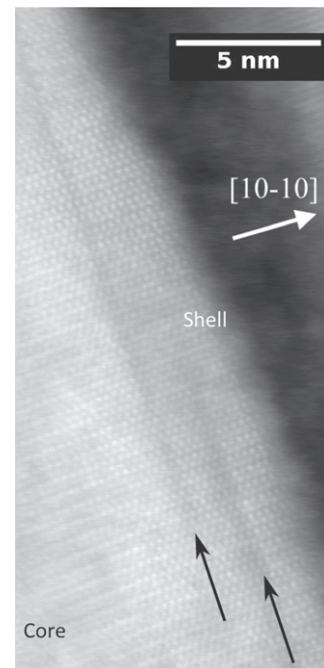


Figure 4. An $\text{In}_{0.5}\text{Ga}_{0.5}\text{N}$ cross-sectional sample showing Ga-rich platelets in the shell (dark linear regions, arrowed), viewed edge-on in a $\{11\text{-}20\}$ direction. These platelets are only 1-2 atomic planes in width.

geometry depends on the orientation of the growth surface and not on specific crystallographic planes. A detailed examination of the (0001) growth surface, as in figure 1(b) also suggests that decomposition into Ga-rich and In-rich platelets extends right to the growth surface, implying that the platelets are formed as growth proceeds rather than through a subsequent ripening process. The decomposition is consistent with thermodynamic calculations which suggest that, at these low growth temperatures, 400–500 °C, $\text{In}_x\text{Ga}_{1-x}\text{N}$ alloys should tend to decompose into Ga-rich and In-rich alloys in

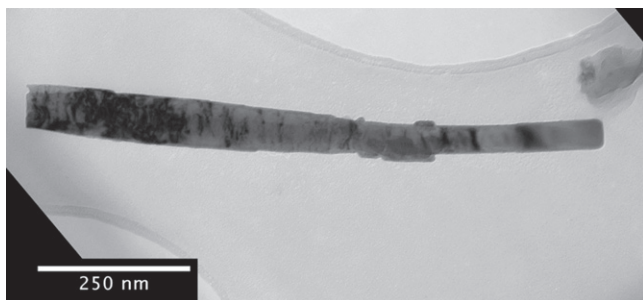


Figure 5. Nanorod graded from $\text{In}_{0.5}\text{Ga}_{0.5}\text{N}$ (left) to InN .

the approximate composition range 0.2 to 0.8 [1]. Such decomposition can be suppressed in alloys grown by MBE under pulsed growth conditions [4]. However, for films grown at a constant rate, STM studies of $\text{In}_x\text{Ga}_{1-x}\text{N}$ films show evidence for segregation into Ga-rich and In-rich islands 1-2 monolayers thick on the (0001) surface [5]. This is much less than the decomposition period in the core (typically up to 6 nm). A possible explanation is that the platelets depend on substantial migration of the In and, perhaps, the less mobile Ga adatoms, which then attach to ledges on the (0001) surface. The observation of the generally In-rich core suggests that In migration from the side-facets is significant. The lateral growth of the In-rich and Ga-rich islands along with some step bunching can then explain both the longer decomposition period and the continuity of the platelets across the nanorods. The observation of semi-polar facets which can be seen on the top surface of most nanorods (figures 1(a) and (b)) provide some further indirect evidence

of the lateral growth process, as lateral growth can account for the extension of these facets in the [0001] direction as nanorod growth proceeds. The platelets observed in the sidewalls, which also extend significantly across the growth surface, might be similarly explained.

Observations of graded specimens provide further insight into the growth mechanism. Figures 5 and 6 are from isolated nanorods from a scraped-off sample, in which the composition has been graded from $x = 0.5$ to $x = 1$, i.e. to pure InN . This was achieved by stepwise increases in the In concentration to $x = 0.625, 0.75, 0.875$ and 1 at 30 min intervals over a 2 h period. Figure 5 shows a general view of a nanorod, taken in a JEOL 2010 TEM. There is decomposition at the left hand end (towards the nanorod base) where $x = 0.5$ and the transition to smooth contrast towards the growth end, which is near pure InN , is indicative of no decomposition. EDX profiles suggested that decomposition into Ga- and In-rich platelets ceased for $x \geq 0.8$. This is consistent with the early thermodynamic calculations by Ho and Stringfellow [1] of the transition from a spinodal to a metastable phase region in the phase diagram, although it should be noted that the phase boundaries are very sensitive to layer strains [6, 7]. Such strains will certainly be present in the thin platelets here. It is also worth noting that there are no threading defects in the nanorod, despite a change of around 5% in the lattice parameters from left to right. Figure 6 shows HAADF, In and Ga maps taken in the JEOL ARM 200F showing a gradual reduction in the Ga content from bottom to top, which correlates with a pronounced tapering of the shell. For average compositions $x \geq 0.8$, a shell was not observed. In contrast, nanorods graded from $x = 0.5$ to $x = 0$, i.e. to pure GaN

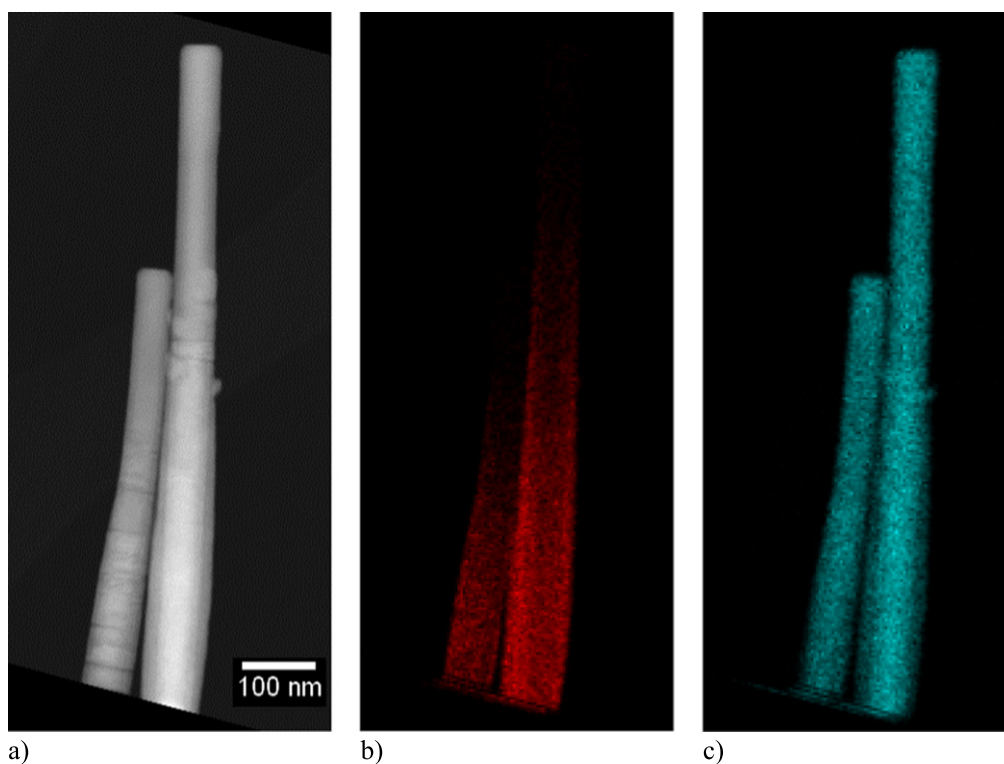


Figure 6. Nanorods graded to InN (a) HAADF, (b) Ga-K map (c) In-L map.

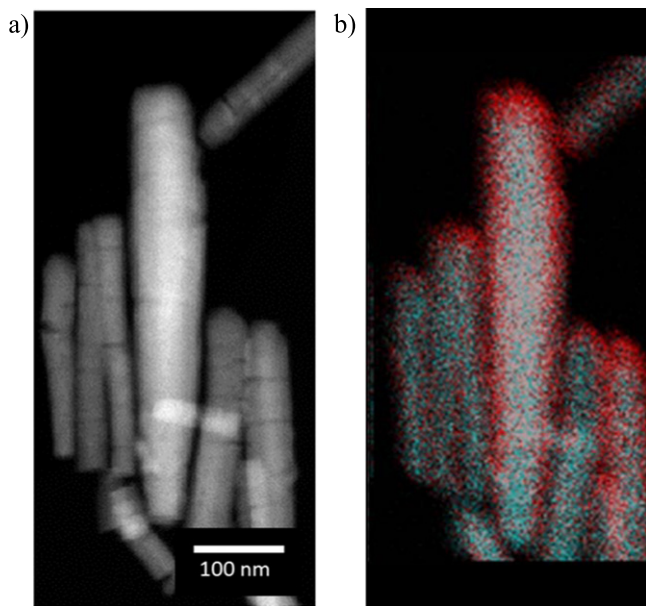


Figure 7. Nanorods graded from $\text{In}_{0.5}\text{Ga}_{0.5}\text{N}$ to GaN, (a) HAADF, (b) combined Ga-K and In-L map (Ga-K and In-L are red and blue respectively).

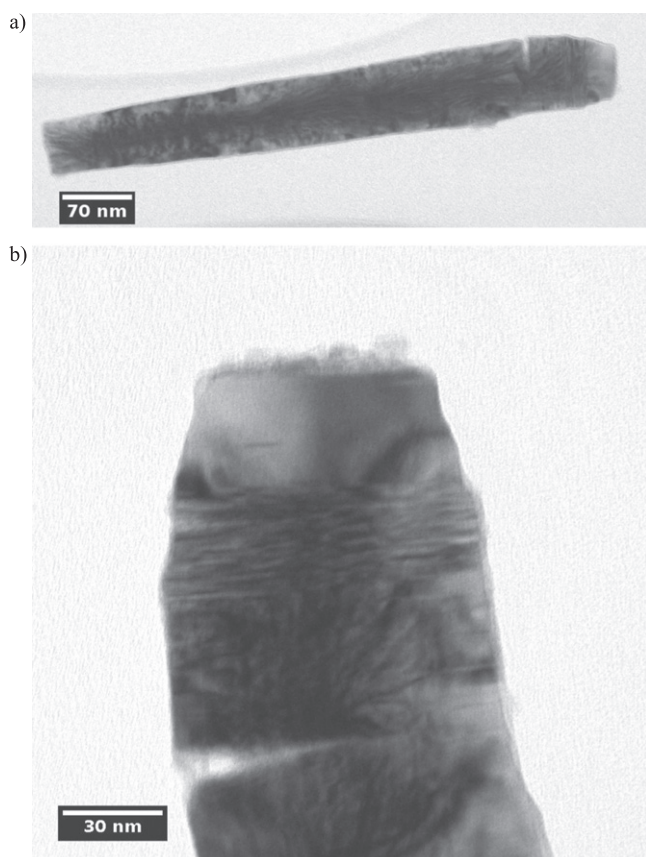


Figure 8. Nanorod graded from $\text{In}_{0.5}\text{Ga}_{0.5}\text{N}$ (left) to GaN shown in (a) and (b) higher magnification of the tip of the nanorod in (a).

showed an increase in the shell thickness, with the core tapering to termination as the In concentration went to zero (figure 7). This shows that the incorporation of the more mobile In adatoms in lateral growth is dependent on the presence of Ga adatoms. Figures 8(a), (b) show that grading to pure GaN produces smooth contrast and thus no evidence of decomposition, at the ends of the nanorods, as in the case of grading to pure InN (figure 5). However, the exact composition at which decomposition ceases for Ga-rich compositions has yet to be determined.

Conclusions

The results here throw new light on the mechanism of core-shell growth outlined in our previous work [3]. The observation of decomposition on {10-10} planes in the shell contrasts with the decomposition in the core, which is on (0001) planes and provides key evidence that the decomposition takes place at the growth surface. The observations can be explained qualitatively by a growth model where In- or Ga-rich islands extend laterally due to surface migration. The observation of nanorods with graded composition have shown that the relative growth rates of the core and the shell change with composition, indicating that the shell can be eliminated for In contents greater than about $x = 0.8$. This transition, which is potentially important for devices, is likely to be dependent on the In migration and desorption rates and thus should be a function of the exact growth conditions.

Acknowledgments

The authors are grateful for the use of the JEOL ARM 200F, South of England Analytical Electron Microscope under EPSRC grant EP/K040375/1 and funding for the growth of nanorods under EPSRC grant EP/I035501/1.

References

- [1] Stringfellow G B 2010 *J. Cryst. Growth.* **312** 735–49
- [2] Cherns D, Webster R F, Novikov S V, Foxon C T, Fischer A M and Ponce F A 2013 *J. Cryst. Growth.* **384** 55–60
- [3] Cherns D, Webster R F, Novikov S V, Foxon C T, Fischer A M, Ponce F A and Haigh S J 2014 *Nanotechnology* **25** 215705
- [4] Fischer A M, Wei Y O, Ponce F A, Moseley M, Gunning B and Doolittle W A 2013 *Appl. Phys. Lett.* **103** 131101
- [5] Chen H, Feenstra R M, Northrup J E, Zywietz T and Neugebauer J 2000 *Phys. Rev. Lett.* **85** 1902
- [6] Gan C K, Feng Y P and Srolovitz D J 2006 *Phys. Rev. B* **73** 235214
- [7] Karpov S Y 1998 *MRS Internet J. Nitride Semicond. Res.* **3** 16